Thermochimica Acta, 138 (1989) 199–206
Elsevier Science Publishers B.V., Amsterdam – Printed in The Netherlands

KINETICS OF SOLID STATE DECOMPOSITION OF $K_3[Nb(O_2)_2F_4]$: TG STUDY

J.K. GHOSH and G.V. JERE

Department of Chemistry, Indian Institute of Technology, Hauz Khas,
New Delhi-110 016 (India)

(Received 17 February 1988)

ABSTRACT

The thermal decomposition of potasium tetrafluorideperoxiniobate(V) ($K_3[Nb(O_2)_2F_4]$) was studied by TG at constant temperature as well as at linearly rising temperatures. The thermal decomposition is regulated by random nucleation and two-dimensional growth mechanism of the nuclei (Avrami–Erofe'ev law). The kinetic parameters obtained at three heating rates (6, 8 and 10 ° C min^{-1}) are in good agreement. However, the kinetic parameters obtained isothermally are smaller than those obtained dynamically.

INTRODUCTION

Solid state isothermal (accumulatary) and photochemical decomposition of fluoroperoxo and tetraperoxo species of transition metals have been reported in earlier publications by the present authors [1–10].

It has been noticed that solid systems which are not associated with water molecules can also be subjected to non-isothermal studies in order to study their kinetic features. Although $K_3[Nb(O_2)_2F_4]$ is a typical coordination compound with large molecular formulation, the only moiety which undergoes decomposition under these conditions is the peroxo group. Hence, this serves as a near-ideal system for kinetic study.

The debate about the pros and cons of both isothermal as well as non-isothermal methods applied to solid state decompositions in order to understand the kinetic features [11–15] prompted the present authors to subject the fluoroperoxo complex $K_3[Nb(O_2)_2F_4]$ to TG study.

EXPERIMENTAL

The solid $K_3[Nb(O_2)_2F_4]$ was prepared by the literature method [1]. It was tested for composition and examined by IR spectra. The relevant data are presented in Table 1.

0040-6031/89/$03.50

TABLE 1

Analysis of $K_3[Nb(O_2)_2F_4]$

	Chemical composition (%)				Weight loss on heating (%) [a]	Characteristic vibrational bands (cm^{-1})
	K	Nb	O_A [b]	F		
Experimental	32.	27.2	8.9	22.3	8.8	890 ν(O–O) 870
Calculated	33.4	2.	9.1	21.7	9.1	590, ν(Nb–F)

[a] TG study.

[b] $O_A = 0.5\ O_2^{2-}$.

The percentage loss in weight observed in the TG study tallies with the peroxy oxygen content (O_A) only. The decomposition is represented as

$$K_3[Nb(O_2)_2F_4](s) \rightarrow K_3NbO_2F_4(s) + O_2(g)$$

The decomposition reaction is exothermic, irreversible and no melting occurs. It falls in the category A(s) → B(s) + C(g). For the kinetic study, the pristine solid was sieved through a 250 μm standard mesh, without initial grinding.

Non-isothermal TG traces were obtained at three heating rates (6, 8 and 10 °C min^{-1}) in a static air atmosphere using STA-781 (Stanton-Redcroft, U.K.). Using the same apparatus and experimental arrangement, a set of isothermal TG traces were obtained for the title solid in the range 483–533 K.

RESULTS

Non-isothermal

In order to obtain reliable kinetic parameters from the rising temperature method (TG study), three heating rates (6, 8 and 10 °C min^{-1}) were employed, and attention was paid to the particle size (250 μm) and small mass (~ 7 mg) of the solid for TG study. Figure 1 shows typical TG traces for the decomposition of $K_3[Nb(O_2)_2F_4]$. Before attempting kinetic analysis using TG curves, the literature procedure for establishing n, the reaction order, an isothermal run (α vs. time) at 533 K, which is in the range of non-isothermal experiment, was analysed using the Avrami–Erofe'ev relation

$$g(\alpha) = -\log(1-\alpha)^{1/n} = kt$$

for $n = 1$, 2 and 3 (Fig. 2). It is seen from Fig. 2 that good linear relationship is observed with $n = 2$.

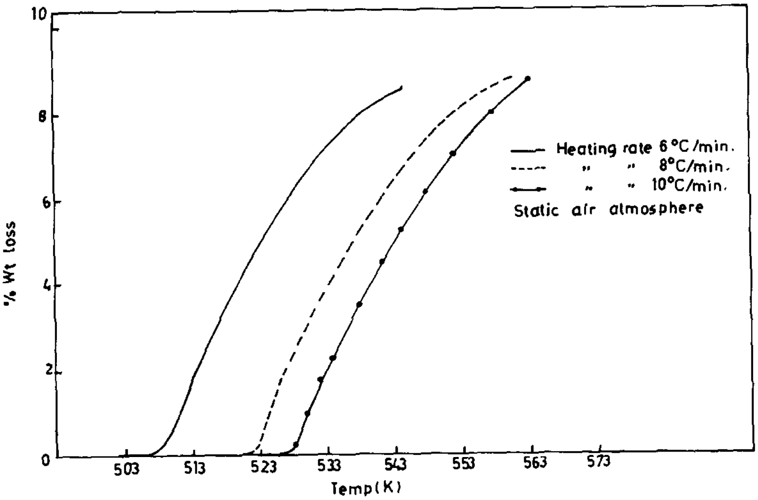

Fig. 1. Thermogravimetric curves for the decomposition of $K_3[Nb(O_2)_2F_4]$ at different heating rates.

The Coats and Redfern method [17] for evaluating the kinetic parameters of a dynamic run is one of the most reliable and commonly employed [18–20]. The following equation is used

$$\log g(\alpha)/T^2 = \log \frac{AR}{\beta E}\left(1 - \frac{2RT}{E}\right) - \frac{E}{2.3RT}$$

where T is the absolute temperature, R is the gas costant, β is the linear

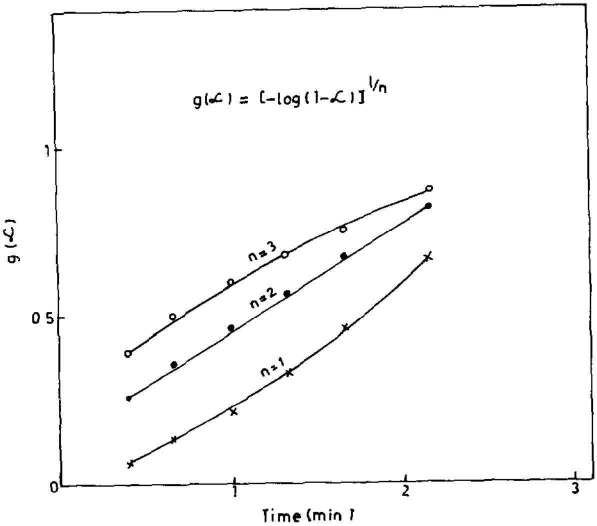

Fig. 2. Plots of g(α) vs. time for the isothermal decomposition of $K_3[Nb(O_2)_2F_4]$ in static air at 533 K.

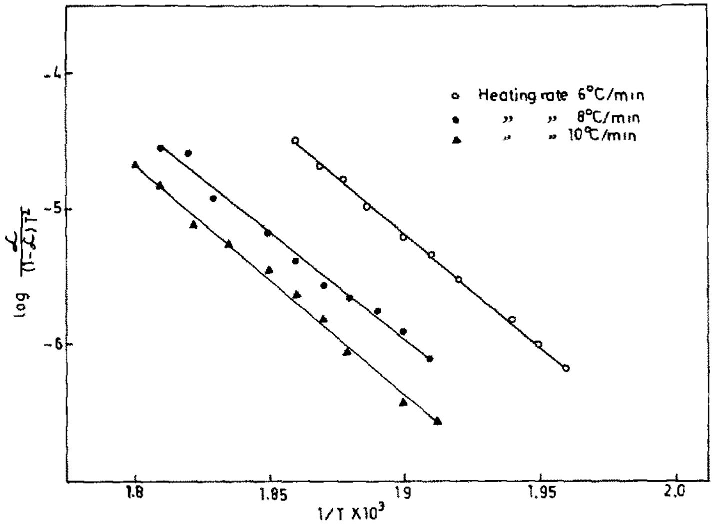

Fig. 3. Plots of log $[\alpha/(1-\alpha)T^2]$ vs. temperature for the decomposition of $K_3[Nb(O_2)_2F_4]$ at different rates (Coats and Redfern [17] method).

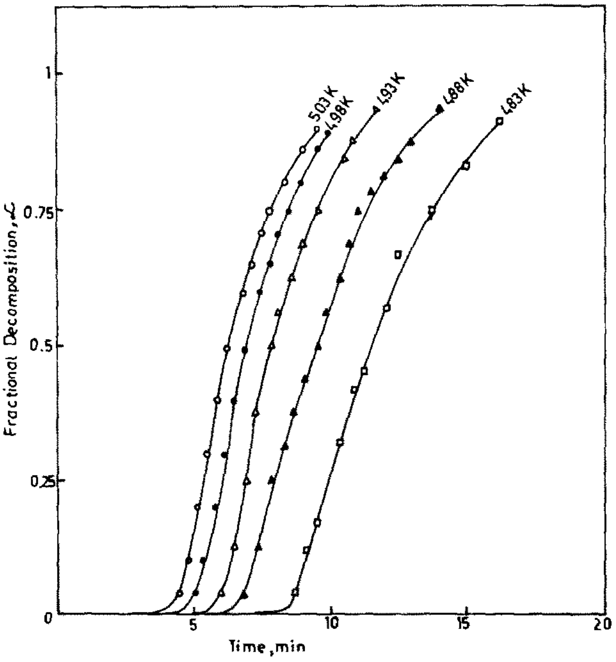

Fig. 4. Isothermal thermogravimetric decomposition of $K_3[Nb(O_2)_2F_4]$.

TABLE 2

Kinetic parameters derived from TG at different heating rates in the α range 0.1–0.9

Heating rate	E (kJ mol^{-1})	log A (s^{-1})
6	295.6	30.2
8	290.7	29.3
10	299.2	29.4

TABLE 3

Kinetic parameters derived from the Arrhenius plots by means of isothermal TG study

	E (kJ mol^{-1})	log A (s^{-1})	$-r$
Avrami–Erofe'ev	82.2	6.2	0.97083
Contracting cube	47.5	2.2	0.96671

heating rate and $g(\alpha) = \alpha/(1-\alpha)$ for $n = 2$. Hence, log $\alpha/(1-\alpha)$ T^2 was plotted against $1/T$ (Fig. 3). Activation energies and frequency factors were calculated from slopes and intercepts respectively, of these plots of three heating rates and are listed in Table 2.

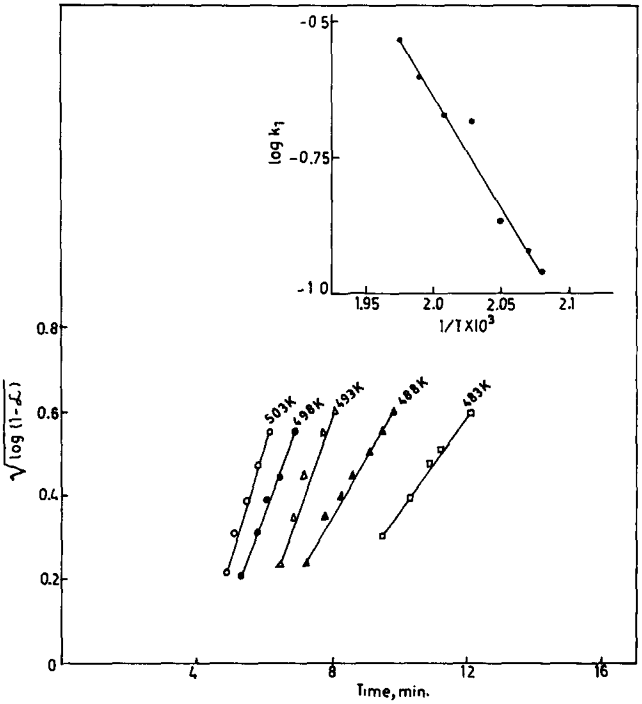

Fig. 5. Plots of the Avrami–Erofe'ev equation for the decomposition of $K_3[Nb(O_2)_2F_4]$. Inset: Arrhenius plot.

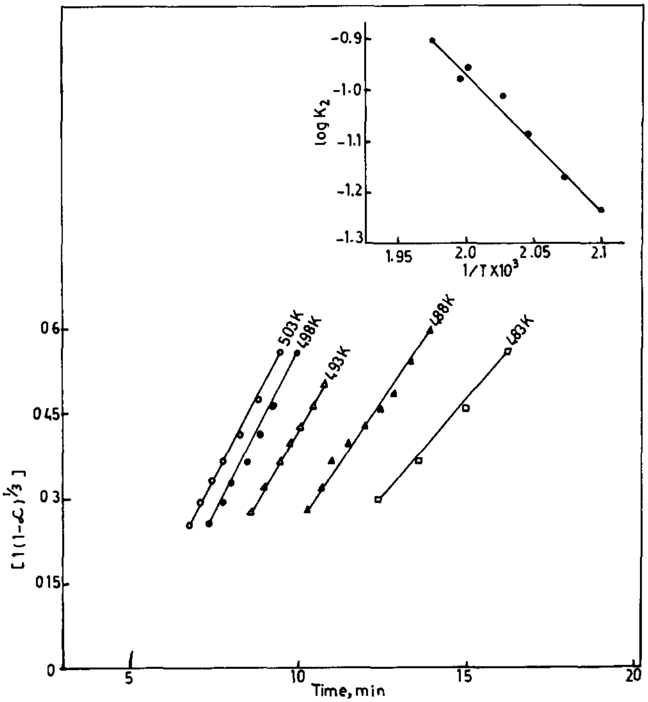

Fig. 6. Plots of the contracting volume equation for the decomposition of $K_3[Nb(O_2)_2F_4]$. Inset: Arrhenius plot.

Isothermal

The α vs. time plots for isothermal TG are given in Fig. 4. The initial part obeys the Avrami-Erofe'ev equation (Fig. 5)

$$-\log(1-\alpha)^{1/2} = k_1 t$$

The latter part obeys the contracting cube equation (Fig. 6)

$$1-(1-\alpha)^{1/3} = k_2 t$$

The kinetic parameters are obtained from slopes and intercepts of respective Arrhenius plots (insets, Figs. 5 and 6) for the above processes and are listed in Table 3.

DISCUSSION

The solid undergoes clean decomposition. It is generally accepted that the reaction mechanism can be elucidated from the isothermal methods, whereas non-isothermal methods present some intrinsic difficulties of their own [21], in addition to the heterogenous nature of decomposition. It is precisely in order to understand these complexities that the authors have subjected the present solid to TG study.

GENERAL OBSERVATIONS ON KINETIC FEATURES OF $K_3[Nb(O_2)_2F_4]$

Isothermal

The Avrami–Erofe'ev equation with $n = 2$ is obeyed in the initial part of the decomposition. This kinetic obedience implies that the solid undergoes decomposition by random nucleation followed by two dimensional growth of the nuclei [22–24]. The later stage of the decomposition is governed by the contracting cube equation. This indicates that the surface has undergone complete decomposition and the interface is advancing towards the centre of the particle. It has been pointed out by Brown and others [22–24] that the α vs. time curves characteristic of the latter part of a reaction, initially obeying the Avrami–Erofe'ev equation, are deceleratory in nature and difficult to analyse completely.

As expected, the E value for the surface process is higher than that of the reaction occurring in the bulk of the solid [22–24], 82.2 and 47.5 kJ mol^{-1} respectively (Table 3).

Non-isothermal

Close agreement is seen between the kinetic parameters obtained at three different heating rates, showing internal consistency (Table 2). It is worth mentioning here that the kinetic parameters obtained from the dynamic TG are considerably larger than those from the isothermal methods (Tables 2 and 3). The difference between the kinetic parameters in the title solid may be tentatively attributed to the decomposition mechanism ($n = 2$). Further work is in progress with other fluoroperoxo and tetraperoxo species of transition metals to understand their kinetic features in a generalized way.

ACKNOWLEDGEMENT

One of the authors (JKG) is grateful to Indian Institute of Technology, Delhi for an award of research fellowship.

REFERENCES

1 G.V. Jere and S.M. Kaushik, J. Thermal Anal., 18 (1980) 277.
2 G.V. Jere and S.M. Kaushik, Thermochim, Acta, 36 (1980) 307.

3 G.V. Jere and S.M. Kaushik, J. Photochem., 12 (1980) 275.
4 G.V. Jere and S.M. Kaushik, J. Solid State Chem., 33 (1980) 145.
5 G.V. Jere, M.K. Gupta, L. Surendra and S.M. Kaushik, Can. J. Chem., 60 (1982) 1891.
6 G.V. Jere, L. Surendra, S.M. Kaushik and M.K. Gupta, Thermochim. Acta, 43 (1981) 379.
7 J.K. Ghosh and G.V. Jere, Photochem. Photobiol., A: Chem., 40 (1987) 295.
8 J.K. Ghosh and G.V. Jere, Thermochim. Acta, 114 (1987) 347.
9 J.K. Ghosh and G.V. Jere, Thermochim. Acta, 117 (1987) 73.
10 J.K. Ghosh and G.V. Jere, Thermochim. Acta, 118 (1987) 229.
11 D.W. Johnson, Jr. and P.K. Gallagher, J. Phys. Chem., 76 (1972) 1474.
12 T.J.W. Bruijn, W.A. Dejong and P.J. Denberg, Thermochim. Acta, 45 (1981) 315.
13 Tong B. Tang and M.M. Chaudhri, J. Therm. Anal., 18 (1980) 247.
14 S.R. Dharwadkar, M.S. Chandrasekhariish and M.D. Karkhanavala, Thermochim. Acta, 25 (1978) 372.
15 Haruhiko Tanaka and Tomoko Sadamoto, Thermochim. Acta, 54 (1982) 273.
16 N. Vuletic' and C. Djordjevic, J. Less-Common Met., 45 (1976) 85.
17 A.W. Coats and J.P. Redfern, Nature (London), 201 (1964) 68.
18 J. Zsako, J. Thermal Anal., 5 (1973) 239.
19 V.M. Gorbachev, J. Thermal. Anal., 8 (1975) 349.
20 H. Tanaka, S. Ohshima, S. Ichiba and H. Negita, Thermochim. Acta, 48 (1981) 137.
21 W.W. Wendladt, Thermal Analysis, 3rd Edn., Wiley-Interscience, New York, 1986.
22 W.E. Brown, D. Dollimore and A.K. Galwey, in C.H. Bamford and C.F.H. Tepper (Eds.), Comprehensive Chemical Kinetics, Vol. 22, Elsevier, Amsterdam, 1980.
23 F.C. Tompkin, Treatise on Solid State Chemistry, Vol. 4, Reactivity of Solids in N.B. Hannay (Ed.), Plenum, New York, London, 1976.
24 W.E. Garner, Chemistry of the Solid State, Butterworths, London, 1955.
25 J.E. House, Jr. and B.J. Smith, J. Inorg. Nucl. Chem., 30 (1977) 777.
26 J.E. House, Jr., R.J. Cardot, D. McCormach and S.E. McCrotty, Trans. 111, State Acad. Sci., 71 (1978) 183.